

21, 489 (1966).

<sup>14</sup>J. Mort, to be published.

<sup>15</sup>Recent magnetoconductivity studies by H. Mell and J. Stuke, private communication, give room temperature mobility values along and perpendicular to the  $c$

axis in excellent agreement with the values measured here.

<sup>16</sup>T. Holstein, Ann. Phys. (N.Y.) 8, 343 (1959).

<sup>17</sup>G. Quentin and J. M. Thuillier, J. Phys. Soc. Japan Suppl. 21, 493 (1966).

## SYMMETRY OF INTERFACE CHARGE DISTRIBUTION IN THERMALLY OXIDIZED SILICON

G. Abowitz, E. Arnold, and J. Ladell  
Philips Laboratories, Briarcliff Manor, New York  
(Received 23 February 1967)

It is well known that the surfaces of  $p$ -type silicon become inverted to  $n$  type upon thermal oxidation. The exact cause of this inversion is not well understood, but it seems to originate in positively charged defects located in the oxide near the oxide-silicon interface. One especially interesting aspect of this phenomenon is that the magnitude of the "built-in" interface charge depends upon the crystallographic orientation of the underlying silicon surface. The orientation dependence of the interface charge has been reported in the literature.<sup>1-5</sup> Of the limited number of orientations investigated, the (111) surfaces exhibit the highest density of charge and the (100) surfaces the least. Several questions immediately arise. What is the generalized dependence of the interface charge upon the crystallographic orientation of the underlying silicon? In particular, is there any other orientation that has still lower values of the interface charge density? In order to answer such questions it is desirable to obtain a more comprehensive orientation dependence of the interface charge. It is the purpose of this Letter to report the results of experiments in which the magnitude of this charge has been determined for all possible crystallographic orientations on one single-crystal specimen. This was accomplished by employing a hemispherical crystal of silicon on which the metal-oxide-semiconductor (MOS) capacitance could be measured for any desired crystallographic direction.

A single crystal of  $6 \Omega \text{ cm}$ ,  $p$ -type silicon was ground and polished to form a perfect hemisphere of approximately 23 mm diameter. The equatorial plane was (111). The hemisphere was oxidized at  $1200^\circ\text{C}$  in dry oxygen to form a  $1500\text{-\AA}$ -thick oxide and slowly cooled to room

temperature. The metallic-blue interference color was observed to be completely uniform over the entire hemisphere. The complete orientation was precisely determined by x-ray techniques on a Philips automatic single-crystal diffractometer (PAILRED).<sup>6</sup> The crystal was then transferred to a goniometer specially constructed to carry out capacitance-voltage measurements on any desired orientation. The field-electrode contact could be made to any point on the oxidized hemispherical surface by means of a mercury drop.<sup>7</sup> The contact to the silicon was made at the equatorial plane. Room-temperature capacitance was measured at 1 kHz and 100 Hz and the results used to obtain the interface charge as a function of the crystallographic orientation.

In the following discussion,  $Q^-$  represents the negative interface charge induced by the "built-in" positive charge located near the interface. The influence of work-function differences is omitted here and will be discussed later. For any given value of charge  $Q_g$  on the field electrode, the interface charge  $Q^-$  is given by

$$Q^- = Q_g + Q_{sc} + Q_t, \quad (1)$$

where  $Q_{sc}$  is the charge in the space-charge region of the semiconductor and  $Q_t$  is the charge trapped in the surface states at the oxide-silicon interface. The distinction between  $Q_t$  and the interface charge is that the former changes with the surface potential while the latter does not. Thus for any given point on the hemisphere, either side of Eq. (1) is a constant for all values of  $Q_g$ . In order to eliminate  $Q_t$  from Eq. (1), the interface charge was determined at the point where the surface potential is ze-

ro, i.e., the Fermi level coincides with the intrinsic level at the surface. At this point  $Q_t$  is also zero if the states in the upper half of the energy gap are acceptors (electron traps), and those in the lower half are donors (hole traps).  $Q^-$  can thus be calculated from Eq. (1), since  $Q_{sc}$  at the desired value of the surface potential is known,<sup>8</sup> and  $Q_g$  corresponding to that surface potential can be obtained from the capacitance-voltage characteristic.<sup>9</sup>

Measurements were carried out systematically over two adjacent 120-deg hemispherical sectors of the surface using a 5-deg grid in both longitude and latitude. Since the [111] direction at the top of the hemisphere is an axis of threefold rotation in the crystal, one 120-deg sector should define the complete crystallographic variation of the measured property if this property complies with crystal symmetry. The values of interface charge density at all grid points were plotted on a stereographic projection<sup>10</sup> of the hemisphere and contours of constant charge density constructed. The results are shown in Fig. 1, in which the positions of several major crystallographic poles are also included.

Figure 1 shows that the  $\langle 111 \rangle$  poles are es-

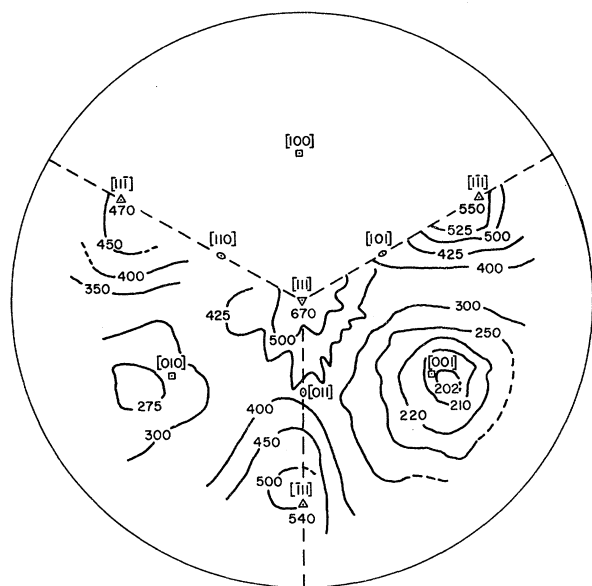


FIG. 1. A [111] stereographic projection showing the variation of the interface charge density with crystallographic orientation for a thermally oxidized silicon single-crystal hemisphere. The values of the constant-charge-density contours are in units of  $10^9 e/cm^2$ . The positions of several major low-index planes are also shown.

entially at maxima, the  $\langle 100 \rangle$  poles at minima, and the  $\langle 110 \rangle$  poles at clearly defined saddle points in the interface charge distribution.<sup>11</sup> Relevant cubic symmetry appears to be manifest. The 120-deg sectors are essentially equivalent in compliance with threefold rotation, and each sector is bisected by a mirror plane. Cubic symmetry also requires that the directional derivatives of a physical property vanish or become infinite at poles which are rotary axes of symmetry, namely the  $\langle 111 \rangle$  threefold rotor and the  $\langle 110 \rangle$  twofold rotors. Thus having established the orientation dependence, it follows that maxima, minima, or saddle points are not likely for any directions in silicon other than those mentioned. This seems to be borne out by Fig. 1. Closer examination of Fig. 1 reveals that the  $\langle 111 \rangle$  and  $\langle 100 \rangle$  poles are slightly displaced from the experimentally observed maximum and minimum positions. Also, there is fine structure in the region of the [111] at the center of the map. Although the reasons for these detailed effects are not understood at the present time,<sup>12</sup> the distribution indicated in Fig. 1 establishes the dependence of the interface charge density on crystal symmetry. Though the oxide is presumably amorphous and defects or impurities in it might be expected to be uniformly distributed, it is clear that the interface charge is directly influenced by the underlying substrate which apparently leaves a strong crystallographic imprint on the interface.

It should be noted that part of the interface charge may originate from work-function differences between silicon and the oxide or the metal electrode. However, the only data presently available indicate that the large variations in interface charge density observed in the present work cannot be accounted for by orientation-dependent work-function differences. The work of Dillon and Farnsworth<sup>13</sup> gives a maximum work-function difference of 0.15 eV between the (100) and (111) faces of silicon, which, in the present work, would correspond to a variation in surface charge density of approximately  $2 \times 10^{10} e/cm^2$ . The observed variation is much greater.

The anisotropy of interface charge, shown in Fig. 1, is strikingly similar to the variation of Young's modulus in silicon. The space group of silicon is  $Fd\bar{3}m$ , which is centrosymmetric; hence, the lowest order tensor property that can display crystal anisotropy is fourth rank.

Elasticity is a fourth-rank tensor<sup>14</sup> with the value of Young's modulus,  $E$ , for a cubic crystal being given by

$$E = [S_{11} - 2(S_{11} - S_{12} - \frac{1}{2}S_{44})(\alpha^2\beta^2 + \beta^2\gamma^2 + \gamma^2\alpha^2)]^{-1}, \quad (2)$$

where  $S_{11}$ ,  $S_{12}$ , and  $S_{44}$  are the three independent elastic compliances, and  $\alpha$ ,  $\beta$ , and  $\gamma$  are the direction cosines of an arbitrary direction based on the cubic axes. The values of the room-temperature compliances are<sup>15</sup>  $S_{11} = 0.768 \times 10^{-12}$  cm<sup>2</sup>/dyn,  $S_{12} = -0.214 \times 10^{-12}$  cm<sup>2</sup>/dyn, and  $S_{44} = 1.26 \times 10^{-12}$  cm<sup>2</sup>/dyn.

If the quantity  $(S_{11} - S_{12} - \frac{1}{2}S_{44})$  is positive, as it is for silicon, the Young's modulus has a maximum in the  $\langle 111 \rangle$  directions and a minimum in the  $\langle 100 \rangle$  directions. The values of  $E$  as a function of orientation were calculated and are shown in Fig. 2, which is a  $[111]$  stereographic projection corresponding to the hemisphere in Fig. 1. The contours of constant  $E$  clearly show the  $\langle 111 \rangle$  maxima,  $\langle 100 \rangle$  minima, and the  $\langle 110 \rangle$  saddle points. In view of the similarity between Figs. 1 and 2, which agree as to major features, it appears that the distribution of interface charge density is governed by a physical property which to the first order is describable by a fourth-rank tensor. The similarity between corresponding maxima, min-

ima, and saddle points in the two figures also suggests that the distribution of interface charge may be related to elastic stresses and strains in oxidized silicon surfaces.

Although the origins of the observed anisotropic interface charge distribution are not clearly understood, a possible mechanism is that the strained regions at the interface act as accumulation areas for point imperfections such as impurity atoms or vacancies. At normal oxidation temperature, for example 1200°C, the defect distribution should be uniform as a result of high mobility at such temperatures. As the specimen is cooled to room temperature, and thermally induced, orientation-dependent strains are built up, these defects may be quenched in and redistributed anisotropically in accordance with these strains. The observation that annealing at 900°C reduces the density of interface charge<sup>16</sup> may thus be explained by stress relief at the interface which is accompanied by a reduction and redistribution of the point defects at the interface as well as by an increase in the structural perfection of the phase boundary.

It may be noted that the rate of thermal oxidation of silicon is best fitted by a mixed linear-parabolic law.<sup>17</sup> The linear term governs the initial surface-controlled rate of growth and is orientation dependent. The parabolic term, which applies to the diffusion-controlled mechanism and is independent of orientation, dominates beyond the initial thin-oxide state. (However, uniform oxide thickness is to be expected over the surface of the hemisphere in the present experiment because of the very large ratio of the orientation-independent to the orientation-dependent rate constants at the oxidation temperature of 1200°C.)<sup>17</sup> One can argue the possibility that the variation of the interface charge density is somehow related to the initial oxide growth mechanism. Since measurements on the MOS system are made after specimens have been cooled to room temperature, however, it is difficult to ascribe the anisotropic interface charge distribution as due primarily to oxide growth factors, since elastic stresses are necessarily introduced upon cooling. Thus, while the oxide growth factors may have some significance in the development of anisotropic interface effects, the strong correlation of the interface charge with crystallographic symmetry, the tensor nature of the measured property, and the fact that

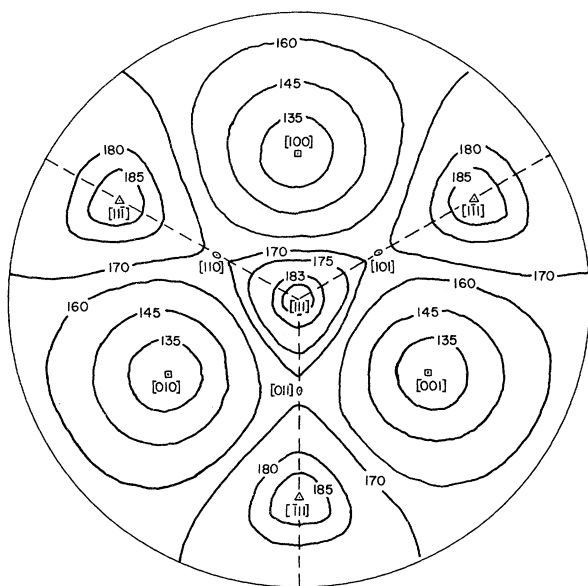


FIG. 2. A  $[111]$  stereographic projection illustrating the variation of Young's modulus,  $E$ , with crystallographic orientation in silicon. The values of the constant- $E$  contours are in units of  $10^{10}$  dyn/cm<sup>2</sup>. The positions of several major low-index planes are also shown.

thermally induced stresses exist suggest that stress and strain may be instrumental in producing the observed interface charge distribution.

The authors are indebted to A. Schoeler, V. Klints, and V. Sapione for their valuable assistance in construction of the experimental apparatus and in carrying out the measurements. Helpful discussions with Dr. F. du Pré and Dr. E. S. Rittner are gratefully acknowledged.

<sup>1</sup>Y. Miura, J. Appl. Phys. (Japan) **4**, 958 (1965).

<sup>2</sup>J. F. Delord *et al.*, Bull. Am. Phys. Soc. **10**, 546 (1965).

<sup>3</sup>P. Balk, P. J. Burkhardt, and L. V. Gregor, Proc. IEEE **53**, 2133 (1965).

<sup>4</sup>E. Kooi, Philips Res. Repts. **21**, 477 (1966).

<sup>5</sup>N. Kawamura and H. Iwasaki, to be published.

<sup>6</sup>J. Ladell, Trans. Am. Cryst. Assoc. **1**, 86 (1965).

<sup>7</sup>G. Abowitz and E. Arnold, Rev. Sci. Instr. **38**, 564 (1967).

<sup>8</sup>A. Many, Y. Goldstein, and N. B. Grover, *Semicon-*

*ductor Surfaces* (John Wiley & Sons, Inc., New York, 1965), Chap. 4.

<sup>9</sup>C. N. Berglund, IEEE Trans. Electron Devices **ED-13**, 701 (1966).

<sup>10</sup>C. S. Barrett, *Structure of Metals* (McGraw-Hill Book Company Inc., New York, 1952), p. 26.

<sup>11</sup>The symbol  $\langle 111 \rangle$  is used generically to include  $[111]$ ,  $[\bar{1}11]$ ,  $[1\bar{1}1]$ ,  $[11\bar{1}]$ , etc., where  $[111]$  denotes the direction normal to the  $(111)$  planes.

<sup>12</sup>One possibility is that the slight shifts result from the fact that the experiment was performed on a hemisphere rather than a full sphere.

<sup>13</sup>J. A. Dillon, Jr., and H. E. Farnsworth, J. Appl. Phys. **29**, 1195 (1958). These authors determined the work function for ion-bombarded silicon in high vacuum. Although these are the best available values, it is not certain that the same values of the work function are applicable to thermally oxidized silicon surfaces.

<sup>14</sup>J. F. Nye, *Physical Properties of Crystals* (Oxford University Press, London, 1957), p. 143.

<sup>15</sup>*American Institute of Physics Handbook* (McGraw Hill Book Company, Inc., New York 1957), p. 3-81.

<sup>16</sup>A. G. Revesz, K. H. Zaininger, and R. J. Evans, J. Phys. Chem. Solids **28**, 197 (1967).

<sup>17</sup>W. A. Pliskin, IBM J. Res. Develop. **10**, 198 (1966).

## POLARIZABILITY OF A TWO-DIMENSIONAL ELECTRON GAS

Frank Stern

IBM Watson Research Center, Yorktown Heights, New York

(Received 13 February 1967)

The response of a two-dimensional electron gas to a longitudinal electric field of arbitrary wave vector and frequency is calculated in the self-consistent-field approximation. The results are used to find the asymptotic screened Coulomb potential and the plasmon dispersion for a plane of electrons imbedded in a three-dimensional dielectric.

There has been increased interest in the theory of two-dimensional systems recently, partly because of the relevance of such theories to the properties of thin films and surfaces. A particularly interesting example is the  $n$ -type inversion layer of a Si-SiO<sub>2</sub>-metal structure, whose density of states has been shown to have the behavior expected of a two-dimensional electron gas,<sup>1</sup> and whose carrier concentration can be varied by at least two orders of magnitude simply by changing the voltage across the oxide layer.

We present results for the response of a two-dimensional electron gas to longitudinal electric fields of arbitrary wave vector  $\vec{q}$  and frequency  $\omega$ , the two-dimensional analog of the longitudinal Lindhard<sup>2</sup> dielectric constant. From this the screening behavior of the sys-

tem, the plasmon frequency as a function of wave vector, and the energy loss of moving charged particles can be calculated. We give as examples the asymptotic expression for the potential due to an external charge, and the approximate solution of the plasmon dispersion equation.

A longitudinal electric field  $\vec{E}(\vec{q}, \omega) = \vec{E}_0 \exp(i\vec{q} \cdot \vec{r} - i\omega t)$  acting on a two-dimensional electron gas will induce a polarization

$$\vec{P}(\vec{q}, \omega) = \chi(\vec{q}, \omega) \vec{E}(\vec{q}, \omega) \delta(z), \quad (1)$$

where  $\vec{q}$  has only  $x$  and  $y$  components,  $\vec{q} \times \vec{E}_0 = 0$ , and the electrons are in the plane  $z = 0$ .

The self-consistent-field treatment of the response of the electron gas gives the same expression for the polarizability  $\chi$  as in the